

Plant Disease Detection Using Generated Leaves Based on DoubleGAN

Yafeng Zhao^{ID}, Zhen Chen^{ID}, Xuan Gao^{ID}, Wenlong Song^{ID}, Qiang Xiong^{ID}, Junfeng Hu^{ID}, and Zhichao Zhang^{ID}

Abstract—Plant leaves can be used to effectively detect plant diseases. However, the number of images of unhealthy leaves collected from various plants is usually unbalanced. It is difficult to detect diseases using such an unbalanced dataset. We used DoubleGAN (a double generative adversarial network) to generate images of unhealthy plant leaves to balance such datasets. We proposed using DoubleGAN to generate high-resolution images of unhealthy leaves using fewer samples. DoubleGAN is divided into two stages. In stage 1, we used healthy leaves and unhealthy leaves as inputs. First, the healthy leaf images were used as inputs for the WGAN (Wasserstein generative adversarial network) to obtain the pretrained model. Then, unhealthy leaves were used for the pretrained model to generate 64*64 pixel images of unhealthy leaves. In stage 2, a superresolution generative adversarial network (SRGAN) was used to obtain corresponding 256*256 pixel images to expand the unbalanced dataset. Finally, compared with images generated by DCGAN (Deep convolution generative adversarial network), the dataset expanded with DoubleGAN, the generated images are clearer than DCGAN, and the accuracy of plant species and disease recognition reached 99.80 and 99.53 percent, respectively. The recognition results are better than those from the original dataset.

Index Terms—GAN, leaf, plant disease detection, superresolution

1 INTRODUCTION

PLANT disease detection and identification tasks have changed greatly from traditional methods to artificial-intelligence methods, and their accuracy has also largely improved. Currently, the best way to use computers to identify plant diseases is through deep learning. For example, deep learning was used for image-based plant disease detection [6]. Fine-tuned deep learning models were developed for plant disease identification [14]. A greenhouse cucumber disease identification system was designed based on a DCNN [7]. An AI-based banana disease and pest detection system was developed using a DCNN to support banana farmers [12]. In addition, a rapid and reliable approach to lesion quantification using image recognition and an artificial neural network model was developed [5]. These methods for recognizing plant diseases have achieved good results. However, deep learning requires a large number of images to train models. A balanced and sufficient dataset for leaf disease detection must contain sufficient

key information for model learning. Small datasets cannot train an effective recognition model, especially datasets with unevenly distributed disease samples, which can easily lead to overfitting. There are thousands of healthy pictures and only a few hundred or even dozens of unhealthy samples, such as those in the PlantVillage database [20]. The problem of uneven sample distribution was mentioned in the PlantVillage database for the study of leaf disease identification and used the methods of flipping and translation to supplement the data set [4]. Compared with regularization and other methods, expanding the original data set can better improve the model performance and prevent overfitting.

Generative adversarial networks (GANs) [3] have been widely studied because they can generate additional data. There are many overview papers on the applications of GANs [2], [15], [18], [19], including image synthesis, semantic image editing, style transfer, image super-resolution and classification, these papers also point to remaining challenges in theory and application of GANs. As a new method to expand data set, GAN can generate high-quality images, it is very useful for image processing. For example, the paper “Unsupervised Representation Learning with Deep Convolutional Generative Adversarial Networks” [20] presents deep convolutional generative adversarial networks (DCGANs) which combines CNN with GANs for unsupervised learning. A method to amplify small sample library based on GAN equivalent model has been proposed [10]. A facial expression recognition method has been proposed based on GAN [16]. An image recognition method has been proposed based on conditional deep convolutional generative adversarial networks [17]. In addition, a semi-supervised generative adversarial networks have been proposed to

- Yafeng Zhao and Zhen Chen are with the College of Information and Computer Engineering, Northeast Forestry University, Harbin 150040, China. E-mail: nefufzy@126.com, czroao@gmail.com.
- Xuan Gao is with the Shenzhen Wanxing Software Co., Ltd, Shenzhen, Guangdong 518000, China. E-mail: gao6754996@163.com.
- Wenlong Song, Junfeng Hu, and Zhichao Zhang are with the College of Mechanical and Electrical Engineering, Northeast Forestry University, Harbin 150040, China. E-mail: {wlSong139, nefuhjf}@126.com, 593257804@qq.com.
- Qiang Xiong is with the China Mobile Communications Group Shanghai Co. Ltd, Shanghai 200060, China. E-mail: 728978493@qq.com.

Manuscript received 22 Sept. 2020; revised 13 Jan. 2021; accepted 31 Jan. 2021.

Date of publication 3 Feb. 2021; date of current version 3 June 2022.

(Corresponding author: Zhen Chen.)

Digital Object Identifier no. 10.1109/TCBB.2021.3056683

TABLE 1
Species and Number of Healthy Leaves

Label	Name	Number
1	Apple	3173
2	Corn	3825
3	Grape	4063
4	Potato	2152
5	Tomato	18757

improve the accuracy of image classification [13]. An image super-resolution (ISR) method has been proposed using generative adversarial networks (GANs) which can increase the resolution of a low-resolution image by 16 times to generate a high-resolution super-resolved (SR) image [8]. Therefore, GAN can be used not only to improve model performance but also to provide endless suitable data.

However, it is difficult to generate large-scale clear images with GAN using a small number of images. The existing dataset of unhealthy plant leaf images is limited in quantity and has an unbalanced distribution of data; therefore, it is easy to collapse for GAN to generate images. For example, although DCGANs can generate small-sized images with high quality [11], when large-scale images are generated by increasing the depth of the model, some problems arise, such as a lack of detail and image blur. The training is not stable, and the loss function does not clearly indicate the training process. To solve these problems, we propose the use of DoubleGAN with images provided by PlantVillage to generate images to expand the unbalanced dataset. First, WGAN was used to input enough healthy leaves to obtain a pretrained model, and a small number of unhealthy samples were input into the pretrained model. A 64*64 pixel image was obtained. We used the Wasserstein distance [1] to optimize the loss function of the original GAN, prevent the model training from collapsing, make the training more stable, and provide a clear training index to the model. Second, SRGAN [9] was introduced to increase the residual network, which not only increased the network depth but also prevented overfitting. The loss function increased the content loss of the generator and prevented the super resolution image from mismatching with the original image. Through SRGAN, clear images of 256*256 pixels were obtained using only a few images. Finally, we combined the new images with the original images and performed classification experiments to judge the effectiveness of the generated images.

2 MATERIAL AND METHODS

2.1 Material

PlantVillage (www.plantvillage.org) is an open database for plant disease diagnosis that includes images of diseased and healthy leaves of various plants. In this paper, 31361 leaf images collected from PlantVillage were used as the experimental data, including healthy leaves from 5 different species and unhealthy tomato leaves affected by 10 diseases. Table 1 shows the species and the numbers of healthy leaves. The minimum number of images for those species is 2152, and the maximum number is 18157. Table 2 lists the diseases and the number of images of tomato leaves with each disease, with 373 images of mosaic virus disease and

TABLE 2
Diseases and the Number of Tomato Leaves With Each Disease
(the Last Row are Healthy Tomato Leaves)

Label	Name	Number
1	bacterial spot	2127
2	early blight	1000
3	late blight	5357
4	leaf mold	952
5	partial leaf spot	1771
6	Two-spotted spidermites	1674
7	target spot	1404
8	mosaic virus	373
9	yellow leaf curl virus	1909
10	healthy	1591

5357 images of late blight disease. The imbalance in the numbers of available leaf images is clear. The samples are shown in Fig 1.

2.2 Method

To generate high-resolution images with clear and detailed information, this paper combines WGAN and SRGAN [22]. The method can be broken down into two stages, as shown in Figs. 2a and 2b. Fig 2a shows the generation of healthy leaves. Fig 2b shows the generation of unhealthy leaves, by using the WGAN trained in Fig 2a as the pretrained model combined with SRAGN. In the first stage, the structure of the generating network and discriminating network is consistent with that of WGAN. The purpose is to obtain 64*64 images with clear and detailed information. In the second stage, the generating network and discriminating network are consistent with that of SRGAN. The purpose is to reconstruct the 64*64 images and then obtain 256*256 high-resolution images with more detailed information. We needed to pretrain the model and then use the parameter values of the pretrained model as the initial value for the model

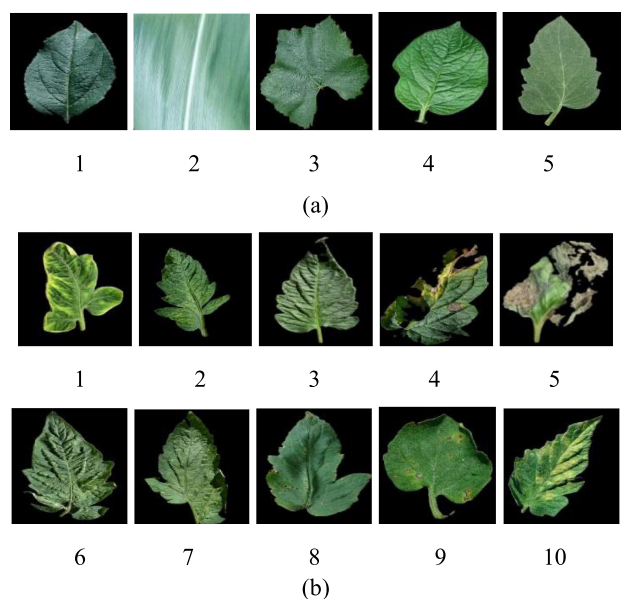


Fig. 1. Leaf samples from healthy plants and diseased tomato plants.
(a) Samples of healthy plant leaves. From 1 to 5 are the leaves of apple, corn, grape, potato and tomato, based on the order in Table 1 (b) Samples of unhealthy tomato leaves. One leaf for each disease, based on the order in Table 2, the last one 10 is a healthy tomato leaf.

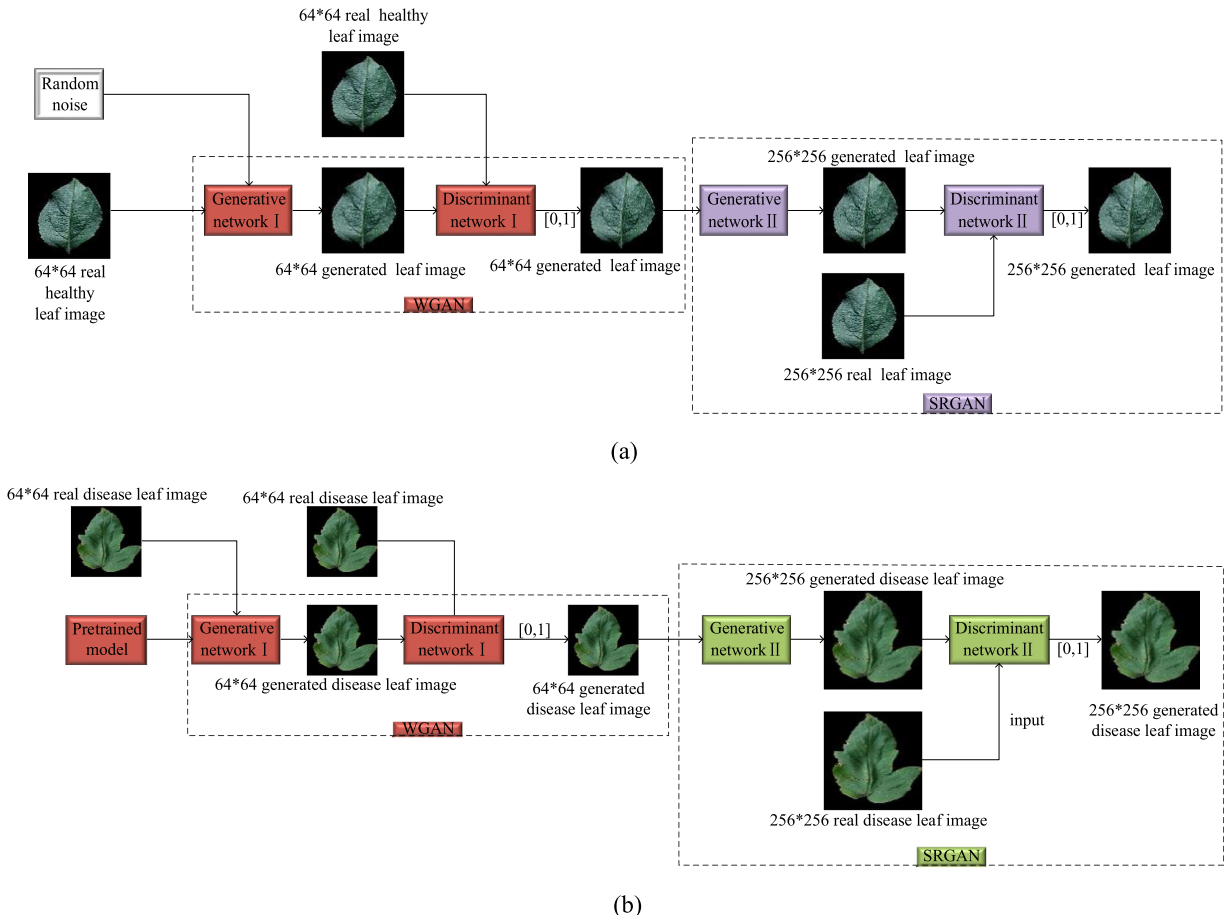


Fig. 2. DoubleGAN structural block diagram. (a) Generation process of healthy leaves (b) Generation process of diseased leaves.

parameters. Some important aspects of this process are:

- The real 256*256 image was downsampled, and the corresponding low-resolution 64*64 image was obtained as the input of the generation network. The generation of the first high-resolution images by superresolution reconstruction was obtained through forward propagation.
- Back-propagation was used to update the network parameters, which allowed the network to reach the global optimal solution.
- When the discriminating network was trained, the discriminating loss was used to calculate the probability that the image generated by the discriminating network came from the natural image domain. If the difference between the obtained probability value and the actual value is smaller, the trained discriminating network is better, and a better discriminating network model was obtained after back-propagation.
- When the generated network was trained, its loss function increased the feature loss compared with that from the traditional GAN, which made up for the lack of high-frequency details in the original mean square error (MSE) loss-generated image. The greater the loss was, the greater the difference between the reconstructed high-resolution image and the real image. After the loss value was obtained, the network parameters were updated through back-propagation to optimize the network

model. The same training carried out for the next batch of images until the global optimal solution was obtained, which made the model converge.

2.2.1 The Principle of DoubleGAN

During training, the WGAN in stage I and the SRGAN in stage II were trained separately. After the model training was completed, random noise was used as the input, and the generated network parts in stage I and stage II were extracted separately and then connected serially.

First Stage of GAN. The first stage of GAN was used to generate a clear, low-resolution 64*64 image. Unlike in the traditional GAN, the loss of the discriminator was the Wasserstein distance between the generated data and the real data, which is defined as:

$$W(P_{\text{data}}, P_G) = \max_{D \in 1-\text{Lipschitz}} \{ E_{x \sim P_{\text{data}}} [D(x)] - E_{x \sim P_G} [D(x)] \}. \quad (1)$$

In (1), x represents the real image from the real data distribution P_{data} ; D represents the discriminant network; G represents the generating network; and E represents the expected value.

A traditional GAN uses JS divergence, in which P_{data} and P_G do not overlap or the overlapping parts can be ignored. JS divergence is always constant, log 2. Therefore, using a gradient descent will lead to gradient disappearance. For the discriminator, the generator loses the gradient information. Even with a near-optimal discriminator, the generator

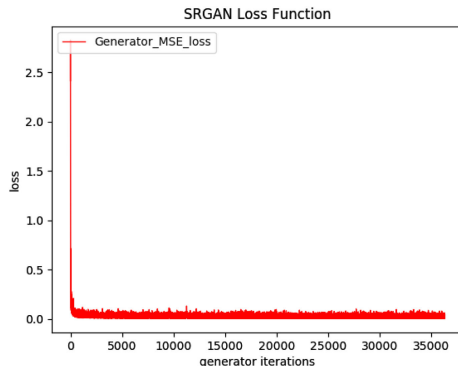


Fig. 3. The change of loss function in the generator pretraining.

may experience gradient disappearance. The Wasserstein distance can solve this problem perfectly. The most obvious advantage of this approach is that even if there is no overlap between P_{data} and P_G , it can still reflect the distance between them. This stabilized the training process and prevented the problem of model collapse caused by the disappearance of the gradient.

Second Stage of GAN. The input images were generated in the first stage. Through the SRGAN, the low-resolution input image is superresolution-reconstructed to obtain clear, high-resolution plant leaf images. GAN aims to minimize perceptual losses through modeling based on MSE, which makes up for the lack of detail. The loss function is formulated as:

$$l^{SR} = l_X^{SR} + al_G^{SR}. \quad (2)$$

In (2), l_X^{SR} represents the content loss; l_G^{SR} represents the adversarial loss; and a represents the adversarial loss weight, which in this experiment is 10^{-3} .

The content loss uses MSE loss to ensure the consistent content between the generated image and the original image. When pixel-level loss occurs between the superresolution image and the real image, the loss is calculated as

$$l_{MSE}^{SR} = \frac{1}{r^2 WH} \sum_{x=1}^{rW} \sum_{y=1}^{rH} (I_{x,y}^{HR} - G(I^{LR})_{x,y})^2. \quad (3)$$

In (3), r represents the down-sampling factor and W, H represent the height and width of the image, respectively. ReLu layer of the pretrained VGG16 was used to compensate for the lack of high-frequency details in the image generated by MSE. Then, the generated image and the matched real image were used as the input for the trained VGG, the characteristic pixels from the middle layer between the two images were extracted, and the euclidean distance between the two images was calculated. The formula is as follows:

$$l_{VGG}^{SR} = \frac{1}{W_{i,j} H_{i,j}} \sum_{x=1}^{W_{i,j}} \sum_{y=1}^{H_{i,j}} \left((\phi_{i,j}(I^{HR}))_{x,y} - (\phi_{i,j}G(I^{LR}))_{x,y} \right)^2. \quad (4)$$

In (4), $W_{i,j}$ and $H_{i,j}$ are the height and width of the extracted feature surface, respectively.

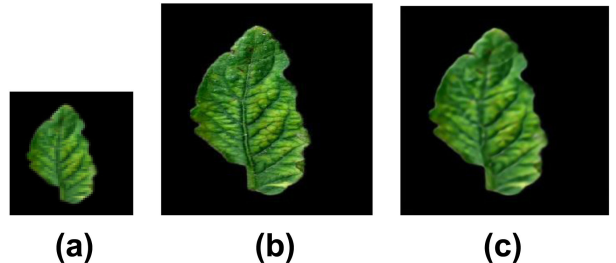


Fig. 4. Superresolution results. (a) Subsampled image, (b) generated high-resolution image, (c) actual high-resolution image.

The adversarial loss was used to ensure that the generated image came from the natural image domain, that is, to ensure that the discriminator could not distinguish whether the image came from the generated image or the real image. As below:

$$l_G^{SR} = \sum_n = -\log D(G(I^{LR})). \quad (5)$$

In (5), $D(G(I^{LR}))$ represents the probability estimation of the discriminator D to the super resolution image $G(I^{LR})$. For better gradient performance, we used $-\log D(G(I^{LR}))$ instead of $\log [1 - D(G(I^{LR}))]$.

2.3 Superresolution Image Generation

First, the generator was pretrained, and the parameters obtained were used as the initial weight of the generator when the SRGAN was trained. The MSE loss function was used to measure the similarity between the superresolution image and the actual image. The higher the similarity was, the smaller the MSE. Fig. 3 shows the change in the loss function in the pretraining process.

It can be seen that pretraining can quickly reduce the error between the generated image and the actual image in a short time. The superresolution results generated by the generator after training are shown in Fig. 4.

2.4 DoubleGAN Generated Image

DoubleGAN divides the building task into two stages. The first stage generates images with a size of 64*64. The second stage generates images with a size of 256*256. The images generated in the first and second stages are shown in Fig. 5.

3 RESULTS AND DISCUSSION

We used the existing generation network DCGAN to generate 256 * 256 images, which were compared with the original images and the images generated by DoubleGAN. The images of unhealthy leaves were used as training data to expand the unbalanced data set. Then, three classical networks, VGG16, ResNet50 and DenseNet121, were used to classify and verify the data set before and after expansion, which proved that the diseased plant leaf image generated by DoubleGAN was very similar to the actual image.

3.1 Images Generated by DCGAN

We used DCGAN to generate 256 * 256 images and compared those images with the images generated by the method proposed in this study. As shown in Fig. 6, the method proposed in this paper results in clearer generated images.

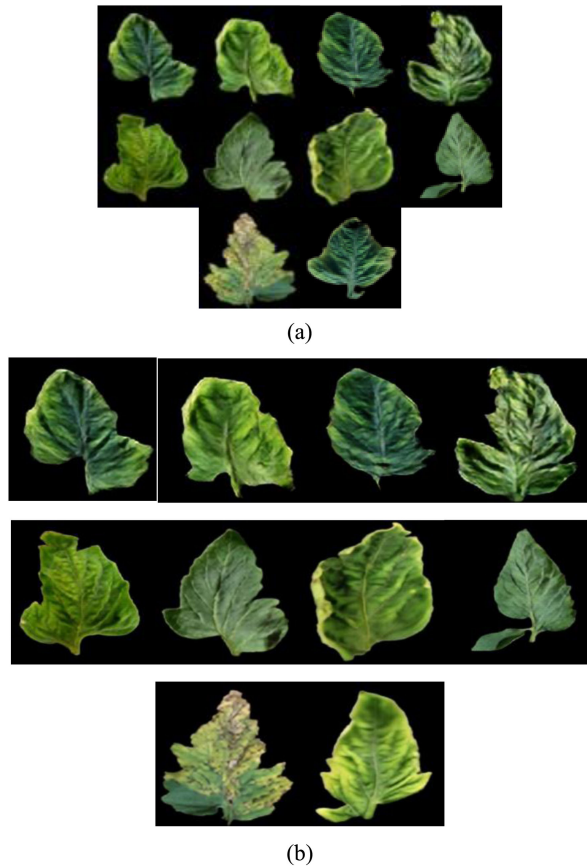


Fig. 5. Images generated by DoubleGAN. (a) DoubleGAN first-stage image generation (b) DoubleGAN second-stage image generation.

3.2 Classification Results for Plant Leaf Images

To objectively evaluate the quality and usability of the generated pictures, we used ResNet50, VGG16 and DenseNet121 to classify the images generated by the traditional method and by DoubleGAN. We first expanded the datasets and then classified the plant species before and after the expansion to verify the practical value of the generated images. The classification results of the test set are represented by a confusion matrix. The abscissa represents the predicted value, the ordinate represents the true value, the diagonal represents the number of correctly identified leaves, and the darker the color is, the more correctly identified leaves there were.

First, the original data set is used for classification. Of the images of 5 kinds of plant leaves (Apple, Corn, Grape, Potato and Tomato), 80 percent were used as the training set and 20 percent were used as the testing set. After 30 epochs using VGG16, ResNet50 and DenseNet121, the confusion matrix of the test set classification results is shown in Fig. 7.

Using rotation and translation, the data set was expanded to 20000 images of 5 kinds of plant leaf images, of which 80 percent were used as the training set and 20 percent were used as the testing set. After 30 epochs using VGG16, ResNet50 and DenseNet121, the classification results for the test set are shown in Fig. 8.

DoubleGAN was used to expand the data set, which had the same number of images and training/test percentages mentioned above. The classification results for the test set are shown in Fig. 9.

Number	Real image	Image generated by DCGAN	Image generated by DoubleGAN
1			
2			
3			
4			
5			
6			
7			
8			
9			
10			

Fig. 6. Images generated by DCGAN and DoubleGAN using real images.

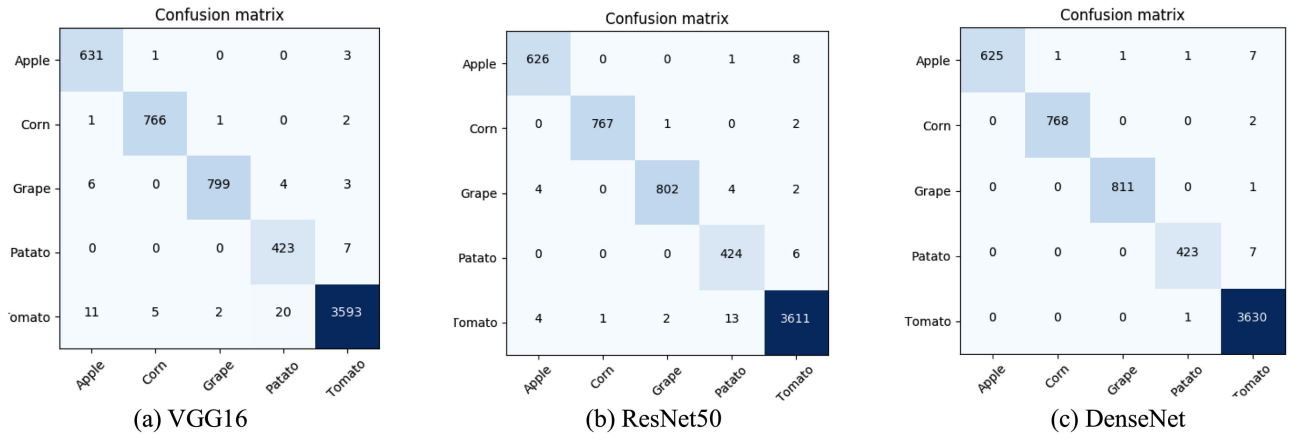


Fig. 7. Classification results of the original plant leaf images data set.

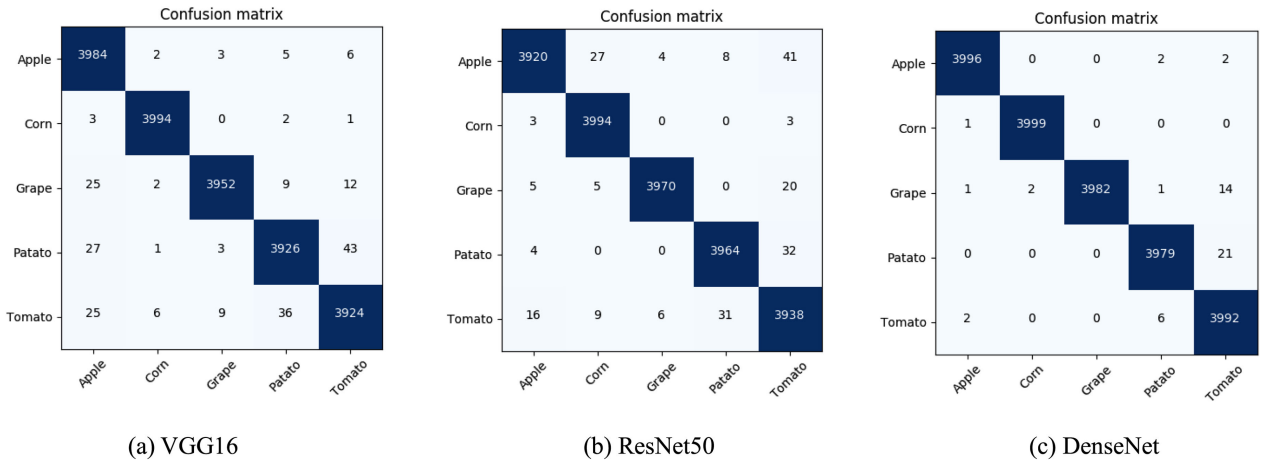


Fig. 8. Classification results of the plant leaf images data set expanded by flipping and translation.

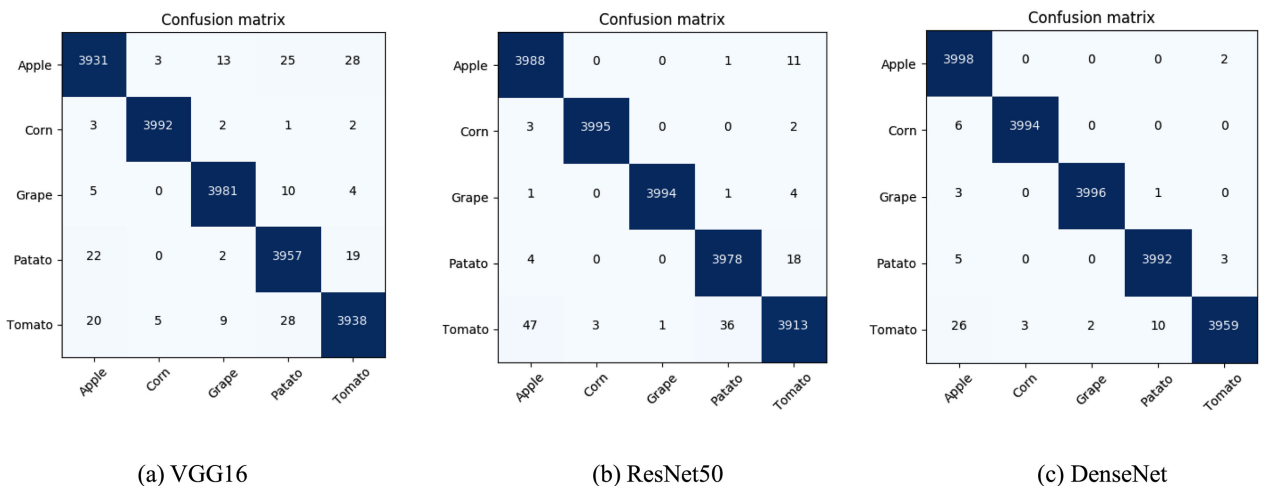


Fig. 9 . Classification results of the plant leaf images data set expanded by DoubleGAN.

The following equation is used to calculate the classification accuracy:

$$ACC = TP / T_x. \quad (6)$$

In (6), TP (True Positive) represents the total number that correctly predict leaf images of each type; T_x (Total x) represents the total number of images of each leaf, where x

represents each leaf type, x can be apple, corn, grape, patato and tomato. For example, T_{Corn} is the total number of corn leaf images. Combined with the above equation and results of confusion matrix, we calculated the classification accuracy of each leaf, shown in Table 3.

The results show that the classification results after the expansion of the dataset by flipping and translation are

TABLE 3
Classification Accuracy of Each Leaf Before and After Data Set Expansion (%)

Species		Apple	Corn	Grape	Potato	Tomato	average accuracy
Original data set	VGG16	99.37	99.48	98.4	98.6	99.45	99.06
	ResNet50	98.58	99.61	98.77	98.6	99.45	99
	DenseNet121	98.43	99.74	99.88	98.37	99.7	99.22
Flipping and translation expansion	VGG16	99.6	99.85	99.8	99.1	98.45	99.36
	ResNet50	98	99.85	99.25	99.1	98.45	98.93
	DenseNet121	99.9	99.98	99.55	99.48	99.8	99.74
DoubleGAN expansion	VGG16	98.28	98.8	99.53	98.45	97.83	98.58
	ResNet50	99.7	99.88	99.85	98.45	97.83	99.14
	DenseNet121	99.95	99.85	99.9	99.8	98.98	99.7

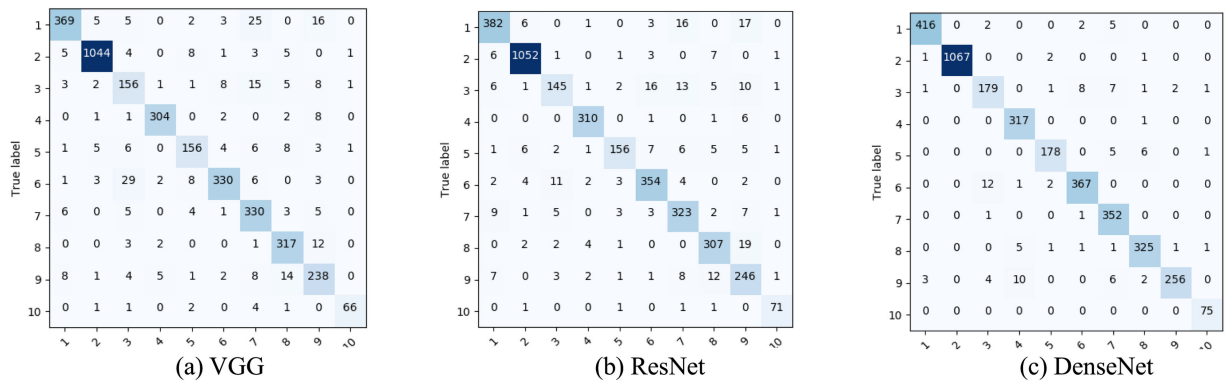


Fig. 10. Classification results of the original tomato leaf images data set.

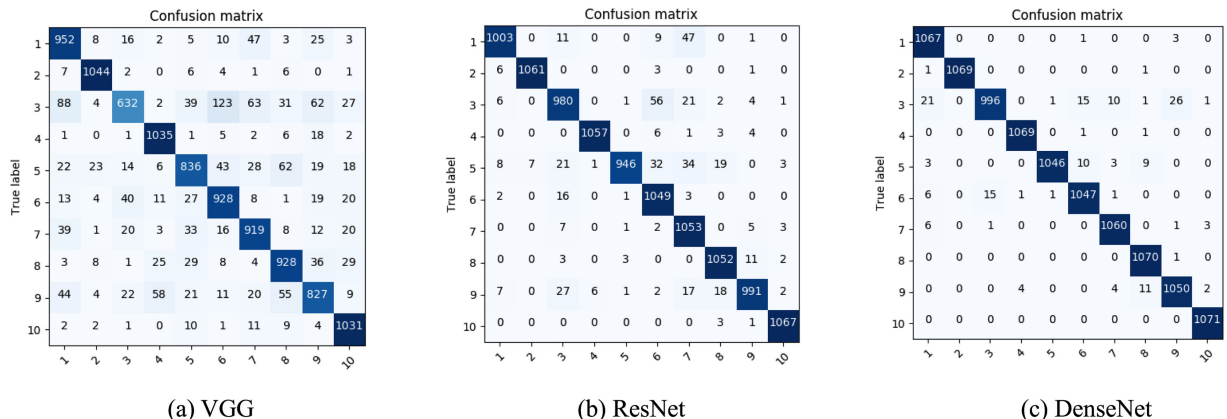


Fig. 11 . Classification results of the tomato leaf images data set expanded by flipping and translation.

slightly better than those before the expansion. The classification accuracy of VGG16, ResNet50 and DenseNet121 on the three different data sets are very close, so the images generated by DoubleGAN are very similar to the original images, and DoubleGAN based on random noise can generate various images which overcome the problem of insufficient diversity caused by the expansion of the original data set just using flipping and translation expansion. Besides, for the recognition accuracy for each plant leaf, the overall classification accuracy for apple, corn, grape and potato was higher than that before the expansion, while the classification accuracy for tomato was

slightly lower than that before the expansion of the data set. Therefore, the experiment shows that using DoubleGAN to generate plant leaf images to expand the dataset has practical value as it can generate various data, so as to solve the problem of unbalanced data set, but there is still a gap between the generated image and the real image.

3.3 Classification Results for Tomato Leaf Images

There were 10 kinds of tomato leaf images. 9 kinds of tomato leaf images with diseased and 1 kind of healthy

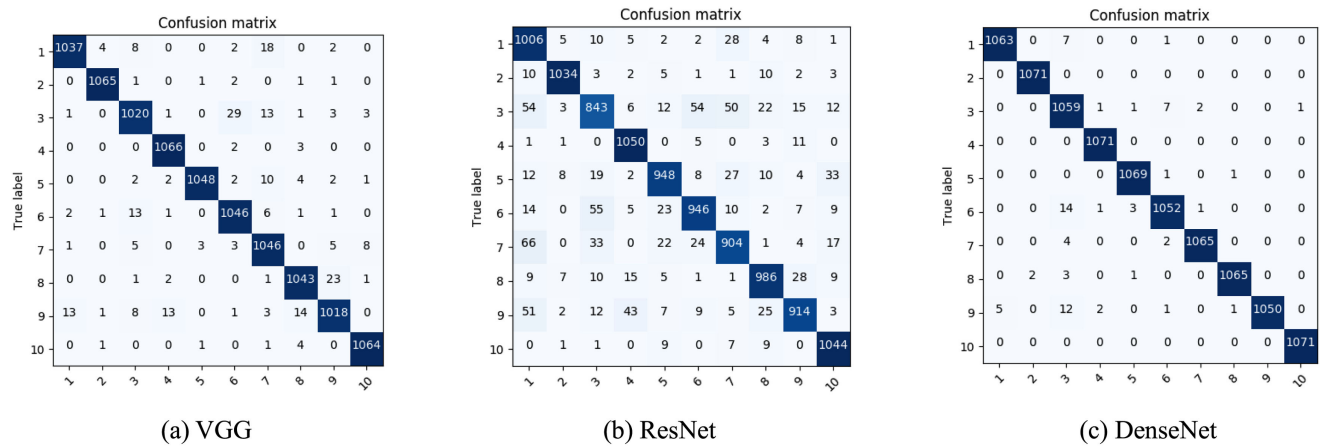


Fig. 12. Classification results of the tomato leaf images data set expanded by DoubleGAN.

tomato leaves (shown in Table 2, Section 2.1), 80 percent were used as the training set and 20 percent were used as the test set. After 30 epochs using VGG16, ResNet50 and

DenseNet121, the classification results from the test set are shown in Fig. 10. The horizontal axis 1 to 10 shows the 10 kinds of tomato leaf images.

Then, the data set was expanded by flipping and translation. The 10 kinds of tomato leaf images in the expanded data set were all 5357 images, with 80 percent as the training set and 20 percent as the test set. After 30 epochs using VGG16, ResNet50 and DenseNet121, the classification results for the test set are shown in Fig. 11.

DoubleGAN was used to expand the data set to the same number of images and training mode as mentioned above. The classification results from the test set are shown in Fig. 12.

The classification accuracy for each leaf type by the three networks before and after the expansions of the data set is shown in Table 4.

Through the comparison, we found that the image similarity of different unhealthy leaves of the same species is higher than the image similarity of leaves of different species and that the differences between different unhealthy leaves can be found in the details. The accuracy of the three networks for disease classification was lower than that for species classification, especially after the expansion of the data set. In the classification of leaf diseases, compared with the classification accuracy for the original images and the flipped and translated images, the classification accuracy for the dataset expanded with DoubleGAN was higher.

4 CONCLUSION

This paper was undertaken to design DoubleGAN for generating plant leaves in order to expand the data set and evaluate the utility of generated leaves by classification accuracy. GAN has been widely used in the field of image generation. However, at this stage, the various GANs proposed by researchers are mainly used to generate images using sufficient samples. In the plant disease database, unhealthy leaves are rare. This study set out to generate 256*256 pixel plant leaf images using small data set, a two-stage GAN named DoubleGAN is proposed.

To evaluate the quality of the generated images, the 256*256 pixel leaf images were used to expand the existing

TABLE 4
Classification Accuracy for Each Leaf Type (%)

Disease	Original data set		
	VGG16	ResNet50	DenseNet121
Bacterial spot	86.82	89.88	97.88
Early blight	78.00	72.50	89.50
Late blight	97.48	98.23	99.63
Leaf mold	83.68	82.11	93.68
Partial leaf spot	93.22	91.24	99.44
Two-spotted spider mites	94.91	91.92	97.31
Target spot	85.00	87.86	91.43
Mosaic virus	88.00	94.67	99.00
Yellow leaf curl virus	86.61	92.91	96.33
Healthy	95.60	97.48	99.69
Flipping and translation expansion			
Disease	VGG16	ResNet50	DenseNet121
Bacterial spot	88.89	93.65	99.63
Early blight	59.01	91.50	92.99
Late blight	97.48	99.07	99.81
Leaf mold	78.06	88.33	97.67
Partial leaf spot	85.81	98.32	98.97
Two-spotted spider mites	86.65	98.23	99.91
Target spot	77.22	92.53	98.04
Mosaic virus	96.27	99.63	100.00
Yellow leaf curl virus	86.65	97.95	97.76
Healthy	96.64	98.69	99.81
DoubleGAN expansion			
Disease	VGG16	ResNet50	DenseNet121
Bacterial spot	93.93	96.83	99.25
Early blight	78.71	95.24	98.88
Late blight	96.55	99.44	100.00
Leaf mold	88.52	97.85	99.81
Partial leaf spot	84.41	97.67	99.44
Two-spotted spider mites	92.06	97.39	99.44
Target spot	85.34	95.05	98.04
Mosaic virus	97.48	99.35	100.00
Yellow leaf curl virus	88.33	97.67	98.23
Healthy	98.04	99.53	100.00

unbalanced data set, and then the expanded data set was used to classify the plant species and diseases with VGG16, ResNet50 and DenseNet121. The results have shown that the classification accuracy for the dataset expanded with DoubleGAN is higher than that for the original dataset and slightly better than that for the dataset expanded by flipping and translation. This means that the generated plant leaf image contains most of the features of the real image. The results of this research support the idea that generated images by GANs can be used to expand the unbalanced dataset. Although the current study is based on a small sample of plant leaves dataset, the findings suggest that the generated image can balance the database. Further work needs to be done to generate higher resolution images with less samples.

ACKNOWLEDGMENTS

We thank Dr. Yafeng Zhao, Dr. Wenlong Song and Dr. Junfeng Hu for excellent technical support. This study was supported by the Fundamental Research Funds for the Central Universities Grants 2572017CB10, 2572019BF09, the Funding of Postdoctoral Research of Heilongjiang Province of China Grant LBH-Z16006.

REFERENCES

- [1] M. Arjovsky, S. Chintala, and L. Bottou, "Wasserstein GAN," 2017, *arXiv:1701.07875v3*.
- [2] A. Creswell, T. White, V. Dumoulin, K. Arulkumaran, B. Bengio, and A. A. Bharath, "Generative adversarial networks: An overview," *IEEE Signal Process. Mag.*, vol. 35, no. 1, pp. 53–65, Jan. 2018.
- [3] G. Ian et al., "Generative adversarial nets," in *Proc. Int. Neural Inf. Process. Syst.*, 2014, pp. 2672–2680.
- [4] S. Jun et al., "Recognition of multiple plant leaf diseases based on improved convolutional neural network," *Trans. Chin. Soc. Agricultural Eng.*, vol. 33, pp. 209–215, 2017.
- [5] B. Li et al., "Rapid, automated detection of stem canker symptoms in woody perennials using artificial neural network analysis," *Plant Methods*, vol. 11, no. 57, 2015.
- [6] S. P. Mohanty, D. P. Hughes, and S. Marcel, "Using deep learning for image-based plant disease detection," *Front. Plant Sci.*, vol. 7, 2016, Art. no. 1419.
- [7] J. Ma et al., "Disease recognition system for greenhouse cucumbers based on deep convolutional neural network," *Nongye Gongcheng Xuebao/Trans. Chin. Soc. Agricultural Eng.*, vol. 34, no. 12, pp. 186–192, 2018.
- [8] D. Mahapatra et al., "Image super resolution using generative adversarial networks and local saliency maps for retinal image analysis," in *Proc. Int. Conf. Med. Image Comput. Comput.-Assist. Intervention*, 2017, pp. 382–390.
- [9] K. Nasrollahi and T. B. Moeslund, "Super-resolution: A comprehensive survey," *Mach. Vis. Appl.*, vol. 25, no. 6, pp. 1423–1468, 2014.
- [10] G. Qiang and J. Zhonghao, "Amplification of small sample library based on GAN equivalent model," in *Electrical Measurement & Instrumentation*, vol. 56, no. 6, pp. 76–81, 2019.
- [11] A. Radford, L. Metz, and S. Chintala, "Unsupervised representation learning with deep convolutional generative adversarial networks," 2015, *arXiv:1511.06434*.
- [12] M. G. Selvaraj et al., "AI-powered banana diseases and pest detection," *Plant Methods*, vol. 15, 2019, Art. no. 92.
- [13] L. Su et al., "General image classification method based on semi-supervised generative adversarial networks," *High Technol. Lett.*, vol. 25, no. 1, pp. 35–41, 2019.
- [14] E. C. Too et al., "A comparative study of fine-tuning deep learning models for plant disease identification," *Comput. Electron. Agriculture*, vol. 161, pp. 272–279, 2018.
- [15] K. F. Wang et al., "Generative adversarial networks: The state of the art and beyond," *Acta Automatica Sinica*, vol. 43, no. 3, pp. 321–332, 2017.
- [16] W. Xiaoqing, W. Xiangjun, and N. Yubo, "Unsupervised domain adaptation for facial expression recognition using generative adversarial networks," *Comput. Intell. Neurosci.*, 2018, pp. 1–10, 2018.
- [17] X. Tang et al., "Image recognition with conditional deep convolutional generative adversarial networks," *Acta Automatica Sinica*, vol. 44, no. 5, pp. 855–864, 2018.
- [18] C. Yinka-Banjo and O. A. Ugot, "A review of generative adversarial networks and its application in cybersecurity," *Artif. Intell. Rev.*, vol. 53, no. 1, pp. 1721–1736, 2019.
- [19] Z. Zeng-Shun et al., "Latest development of the theory framework, derivative model and application of generative adversarial," *J. Chin. Comput. Syst.*, vol. 39, no. 12, pp. 2602–2606, 2018.
- [20] D. P. Hughes and M. Salathé, "An Open Access Repository of Images On Plant Health to Enable the Development of Mobile Disease Diagnostics," 2015, *arXiv:1511.08060*.
- [21] A. Radford, L. Metz, and S. Chintala, "Unsupervised representation learning with deep convolutional generative adversarial networks," in *Proc. Int. Conf. Learn. Representations*, 2016, pp. 1–16.
- [22] C. Ledig et al., "Photo-realistic single image super-resolution using a generative adversarial network," in *Proc. IEEE Conf. Comput. Vis. Pattern Recognit.*, 2017, pp. 4681–4690.



Yafeng Zhao received the master's degree in control theory and control engineering from Harbin Engineering University, in 2006, and the PhD degree in forestry engineering from Northeast Forestry University, in 2016. From 2017 to 2018, she worked as a visiting scholar at Ohio State University. Currently She is an associate professor and master tutor with the College of Information and Computer Engineering of Northeast Forestry University. Her research interests include computer vision and pattern recognition, artificial intelligence and intelligent control, wireless sensor networks. She has published more than 20 academic papers in SCI, EI source journals and Chinese core journals, authorized more than 10 invention patents and utility model patents, presided over and participated in more than 10 provincial and ministerial projects such as the National Natural Science Foundation of China and Heilongjiang Natural Science Foundation, and published two works as chief editor.



Zhen Chen received the bachelor's degree in electronic information engineering from Hubei Polytechnic University, in 2019. He is currently working toward the graduate degree in electronic and communication engineering at Northeast Forestry University. His main research interests include computer vision, object detection, and semantic segmentation.



Xuan Gao received the master's degree in forestry engineering automation from Northeast Forestry University, in 2020. She is currently working with Shenzhen Wanxing Software Co., Ltd, China. She has three publications in SCI, EI source journals and Chinese core journals, and one patent. Her main research interests are image classification and tree species identification.



Wenlong Song received the PhD degree in mechanical design and theory from Northeast Forestry University, in 2008. He is currently vice president of Northeast Forestry University, professor and doctoral supervisor of the College of Mechanical and Electrical Engineering of Northeast Forestry University. His research interests include detection technology of plant life information, detection and control technology of forestry engineering processing process and mechatronics control technology. He has presided more

than 10 National Natural Science Foundation of China, Ministry of education new century talent support plan, Heilongjiang Province Science and technology research project, Harbin Science and technology research project, and Central University Scientific Research Fund project. He has published more than 30 scientific and technological articles, edited two teaching materials and won one second prize of Heilongjiang Province Science and technology progress award. He also serves as a standing member of forestry machinery branch of China forestry society, standing director of forest engineering branch of China forestry society, member of measuring instrument Professional Committee of China Measurement and testing society, and director of Heilongjiang automation society.



Qiang Xiong received the master's degree in electronics and communication engineering from Northeast Forestry University, in 2019. His master's thesis Research on Leaf Formation Method of Diseased Plants Based on Generative Adversarial Network was rated as excellent. He is currently working at China Mobile Communications Group Shanghai Co. LTD, China. His main research interests are artificial intelligence and generative adversarial network.



Junfeng Hu received the bachelor's degree in automation from Harbin Engineering University, in 2003, the master's degree in control theory and control engineering from Northeast Forestry University, in 2008, and the doctor's degree in forestry engineering from Northeast Forestry University, in 2015. He is an associate professor and master supervisor with the College of Mechanical and Electrical Engineering, Northeast Forestry University. His research interests include deep learning, intelligent control, image processing,

and pattern recognition. From 2017 to 2018, he worked as a visiting scholar at Ohio State University in the United States. He has presided over a number of provincial-level and ministerial-level projects such as the Provincial Natural Science Fund, the provincial postdoctoral program, and the central University business special project. He has compiled one teaching material, published more than 10 SCI, EI and core papers, and authorized four patents.



Zhichao Zhang received the bachelor's degree in automation from the Qingdao University of Science and Technology, in 2019. He is currently working toward the graduate degree in control science and engineering in Northeast Forestry University. His research interests include computer vision, image processing, and image classification.

▷ For more information on this or any other computing topic, please visit our Digital Library at www.computer.org/cSDL.